mAbs 6:6, 1518–1532; November/December 2014; © 2014 Amgen Inc.

Russell body phenotype is preferentially induced by IgG mAb clones with high intrinsic condensation propensity: Relations between the biosynthetic events in the ER and solution behaviors in vitro

Haruki Hasegawa[1,*], Christopher E Woods[2], Francis Kinderman[3], Feng He[2], and Ai Ching Lim[1]

[1]Department of Therapeutic Discovery; Amgen; Seattle, WA USA; [2]Department of Drug Product Development; Amgen; Seattle, WA USA; [3]Department of Product Attribute Sciences; Amgen; Thousand Oaks, CA USA

Keywords: crystalline body, endoplasmic reticulum, gelation, immunoglobulin, phase separation protein aggregation, protein condensation, protein crystallization, Russell body

Abbreviations: BFA, Brefeldin A; CB, crystalline body; DIC, differential interference contrast; ER, endoplasmic reticulum; Fab, fragment antigen binding; HC, heavy chain; HEK, human embryonic kidney; IgG, immunoglobulin G; LC, light chain; mAb, monoclonal antibody; RB, Russell body; VH, heavy chain variable domain; VL, light chain variable domain.

The underlying reasons for why some mAb (monoclonal antibody) clones are much more inclined to induce a Russell body (RB) phenotype during immunoglobulin biosynthesis remain elusive. Although RBs are morphologically understood as enlarged globular aggregates of immunoglobulins deposited in the endoplasmic reticulum (ER), little is known about the properties of the RB-inducing mAb clones as secretory cargo and their physical behaviors in the extracellular space. To elucidate how RB-inducing propensities, secretion outputs, and the intrinsic physicochemical properties of individual mAb clones are interrelated, we used HEK293 cells to study the biosynthesis of 5 human IgG mAbs for which prominent solution behavior problems were known a priori. All 5 model mAbs with inherently high condensation propensities induced RB phenotypes both at steady state and under ER-to-Golgi transport block, and resulted in low secretion titer. By contrast, one reference mAb that readily crystallized at neutral pH in vitro produced rod-shaped crystalline bodies in the ER without inducing RBs. Another reference mAb without notable solution behavior issues did not induce RBs and was secreted abundantly. Intrinsic physicochemical properties of individual IgG clones thus directly affected the biosynthetic steps in the ER, and thereby produced distinctive cellular phenotypes and influenced IgG secretion output. The findings implicated that RB formation represents a phase separation event or a loss of colloidal stability in the secretory pathway organelles. The process of RB induction allows the cell to preemptively reduce the extracellular concentration of potentially pathogenic, highly aggregation-prone IgG clones by selectively storing them in the ER.

Introduction

Although the vast majority of antibodies are known to be highly soluble in aqueous solution, there are groups of immunoglobulins that show remarkable phase behaviors such as crystallization, aggregation, liquid-liquid phase separation, gelation, and fibril formation.[1-7] While it is difficult to determine what percentage of immunoglobulin clones in a given repertoire exhibits such high protein condensation propensities, every individual is believed to carry those immunoglobulins in circulation.[6] However, they are normally harmless (thus asymptomatic) because their overall concentrations are usually low,[8] unless over-produced as paraproteins in the advanced stages of multiple myeloma and other plasma cell dyscrasias where serum IgG concentration can exceed 70 mg/ml.[9]

Extensive variations in the intrinsic net attractive inter-protein interaction energy (due to diverse surface charge distribution patterns unique to each mAb clone) have been proposed as an underlying cause for the solution behavior differences among distinct monoclonal antibodies (mAbs).[3,10] Similarly, differential susceptibility to various types of physical stresses appears to originate from the preexisting stability variations inherent to

*Correspondence to: Haruki Hasegawa; Email: harukih@amgen.com; h.haruki@gmail.com
Submitted: 07/28/2014; Revised: 08/22/2014; Accepted: 08/25/2014
http://dx.doi.org/10.4161/mabs.36242

individual mAb clones.[11,12] Given the sequence diversities in the variable regions of immunoglobulin molecules, some IgG mAb clones are bound to possess prominent aggregation property and stress-susceptibility a priori. Such predisposed propensity then manifests itself whenever the right conditions are presented. But otherwise, such propensities would remain latent. While the different solution behaviors of distinct IgG clones must originate from the interplay between the intrinsic properties embedded in the molecule itself and the various extrinsic environmental parameters, the accurate prediction of such behaviors remains difficult despite its importance in biopharmaceutical manufacturing[13] and in the pathogenesis of immunoglobulin deposition diseases.[6,14]

Episodes of immunoglobulin condensation during protein biosynthesis can lead to the formation of Russell body (RB), enlarged globular aggregates of immunoglobulins stored in the endoplasmic reticulum (ER), both in homologous and heterologous cellular systems.[15,16] Depending on the differences in physicochemical properties embedded within the variable regions of heavy chain (HC) and light chain (LC), some human IgG clones readily aggregate into RB in the ER lumen, whereas other IgG clones are much less prone to induce RB under the same expression conditions.[6,15] However, the underlying biophysical or biochemical basis for why some IgG clones are far more inclined to aggregate into RBs remains elusive. Likewise, while RB phenotypes have been extensively studied at the cellular level,[15-18] little is known about the characteristics of the RB-inducing IgG mAb clones after secreted from the cells. Indeed, it is poorly understood whether there are any physiologically relevant differences in aqueous solution behaviors between RB-inducing IgG mAb clones and generic innocuous IgG mAb clones.

To explore the link between the intrinsic physicochemical properties of IgG mAb clones and the phenotypes of the cells that overexpress them, we examined the early biosynthetic events of full-length human IgG mAb clones for which high intrinsic aggregation propensities were known a priori. Specifically, we selected (*i*) 2 IgG2κ mAbs with marked low solubility at neutral pH, (*ii*) 2 IgG2κ mAbs with pronounced sensitivity to mechanical agitation stress, and (*iii*) one IgG2κ mAb with exceptionally high solution viscosity. As references, we tested (*iv*) one IgG2κ mAb that was previously shown to crystallize readily at neutral pH environments both in vitro and in vivo[19] and, lastly, (*v*) one IgG1κ mAb without readily identifiable solution behavior issues. In order to compare the phenotypes of the cells under equivalent conditions, the HC and LC coding sequences were expressed from episomally maintained expression vectors transiently transfected into HEK293 cells. This approach revealed that the intrinsic physicochemical properties of individual mAb clones differently influenced the biosynthetic events in the ER, and thereby induced distinct cellular phenotypes and affected the secretory output. RB formation thus appeared to represent a phase separation event or a loss of colloidal stability that precipitously took place in the secretory pathway organelles. The induction of RB phenotypes can therefore be the earliest tangible evidence by which we can distinguish intrinsically aggregation-prone IgG mAb clones from innocuous generic mAbs. Relationships of IgG mAb behaviors in vitro and in cellulo, potential values of cell phenotype screening in therapeutic lead candidate selection, and the implications for the physiological roles of RB formation in vivo are discussed.

Results

RB phenotype is induced by a human IgG2κ (mAb-A) that has intrinsic propensity to gel at neutral pH environment

For the 5 model human IgG mAbs (clones A–E) and 2 reference mAbs (clones F and G), the target antigen class, the germline gene segment usage for VH and VL, calculated isoelectric point, and the types of known solution behavior issues are summarized in **Table 1**. We did not find apparent association of specific sequence-based attributes to particular solution behavior issues in this antibody panel.

The first model mAb (mAb-A) was marked by its low solubility at neutral pH range. This propensity was identified during the characterization of pharmaceutical properties during an early development stage. While mAb-A was completely soluble at 70 mg/ml in a buffered pH 5.0 condition (**Fig. 1A-1**), mAb-A solution immediately turned gel-like and opaque when the solution pH was raised to a neutral range (**Fig. 1A-2**). The gel remained at the bottom of the vial even when the glass vial was placed upside down (**Fig. 1A-3**). When a smear of the gel was viewed with a DIC microscope, the gelated material was composed of slurry of heterogeneously condensed protein globules (**Fig. 1B**). No other major issues were identified.

Co-transfection of HC- and LC-encoding expression constructs into HEK293 cells resulted in the secretion of fully assembled IgG (**Fig. 1C** left and middle panels, lane 1). By contrast, a separate transfection of individual subunit chains resulted in no detectable protein secretion despite the protein synthesis (**Fig. 1C**, middle and right panels). The LC subunits are often secreted by itself in the absence of HC expression. However, our previous studies showed that there are LC clones that are at odds with this consensus view.[15] Typically, those LCs have high aggregation propensities and induce RBs by themselves (see below). In a 7-day batch cell culture method (see Materials and methods), the secretion titer of mAb-A was around 10 mg/L on average (**Table 2**). Given that the secretion output can reach 300 mg/L in this expression system, the secretion level of mAb-A was clearly on the lower end of the range. In this expression system, cell viability and viable cell density can vary during the course of the 7-day cell culture process depending on the RB-inducing propensities of the overexpressed mAb clone.[15] However, cell viabilities at 72 hr post transfection were mostly greater than 85% when the imaging studies were carried out. The cell viability data for a representative experiment of each mAb clone were provided in the corresponding figure legend.

Under normal cell growth conditions, RB phenotype was induced in 18.6% of the transfected cells (**Fig. 1E**, first row; **Table 2**). When the cells were cultured in the presence of Brefeldin A (BFA), a widely used inhibitor of ER-to-Golgi transport,[20,21] the IgG secretion was effectively blocked during the

Table 1. Characteristics of 7 model human IgG mAb clones evaluated in this study. For the fourth and fifth columns, the identity (in percentage) to the corresponding germline sequence is shown on a gene-segment-by-gene-segment basis

mAb	Antigen class	HC sublcass / LC isotype	V-D-J gene usage for VH (identity to germline)	V-J gene usage for VL (identity to germline)	Calculated isoelectric point	Identified unfavorable solution properties
A	cytokine receptor	G2 / kappa	VH4|4-59/D3|3-22|RF2/JH2 (91.8%/33.3%/93.8%)	VK3|A27/JK1 (89.4%/92.3%)	pH 8.93	low solubility at neutral pH
B	integrin	G2 / kappa	VH3|3-11/D6|6-19|RF1/JH4 (96.9%/80.0%/100%)	VK1|L19/JK1 (94.6%/100%)	pH 8.39	low solubility at neutral pH
C	cytokine receptor	G2 / kappa	VH1|1-24/D3|3-3|RF2/JH4 (92.9%/33.3%/86.7%)	VK2|A2/JK4 (96.9%/100%)	pH 6.58	agitation sensitivity
D	growth factor receptor	G2 / kappa	VH1|1-18/D3|3-3|RF3/JH4 (100%/40%/93.3%)	VK4|B3/JK3 (97.0%/100%)	pH 7.0	agitation sensitivity
E	cytokine receptor	G2 / kappa	VH1|1-24/D6|6-6|RF1/JH4 (96.9%/70%/93.3%)	VK4|B3/JK1 (93.9%/100%)	pH 6.33	high viscosity
F	secreted factor	G2 / kappa	VH1|1-18/D7|7-27|RF1/JH6 (83.7%/33.3%/73.7%)	VK1|O2/JK4 (90.3%/92.3%)	pH 7.05	crystallization at neutral pH
G	secreted factor	G1 / kappa	VH3|3-48/D4|4-17|RF2/JH4 (92.9%/60%/80%)	VK2|A19/JK2 (99.0%/92.3%)	pH 8.51	no notable issues

24-hr treatment period (**Fig. 1D**) and, due to the accumulation of IgG in the ER, the prevalence of RB-positive cells increased to 37.5% (**Fig. 1E**, second and third rows; **Table 2**). For the HC-only and LC-only transfected cells, the RB phenotype frequency was 65.8% and 90.6%, respectively (**Fig. 1F**; **Table 2**).

RB phenotype frequency was much higher when the subunit chains were expressed individually (HC alone, 65.8%; LC alone, 90.6%) than when they were co-expressed (18.6%). Apparently, the high aggregation propensities of individual subunit chains were alleviated by the interactions and assembly of the 2 subunit chains. However, as is clear from our past[15,22] and present study (below), every IgG clone is unique when it comes to the RB-inducing propensity of individual subunit chains and it is not yet possible to derive a rule whether RB-inducing propensities are to increase or decrease by the co-expression of HC and LC subunits.

Induction of RBs during the overexpression of human IgG2κ (mAb-B) that exhibits pH- and temperature-dependent needle-shaped particulate formation

The second IgG model clone (mAb-B) also presented low solubility issues at neutral pH range. Although mAb-B was soluble at 70 mg/ml in an acidic pH solution (**Fig. 2A**, left), the mAb-B solution instantly became clouded upon shifting the pH to a neutral range (**Fig. 2A**, middle). When microscopically examined, the clouded solution was filled with short needle-like particulates (**Fig. 2B**). The needles, however, did not settle to the bottom of the vial by gravity even after a static incubation at room temperature for 24 hrs. Interestingly, incubation at 4°C restored the solubility of mAb-B at neutral pH (**Fig. 2A**, right). No other marked solution behavior problems were identified for mAb-B.

Co-transfection of HC and LC constructs into HEK293 cells led to the secretion of fully assembled IgG (**Fig. 2C** left and middle panels, lane 1). When individual subunit chains were independently expressed, a small amount of LC monomers and LC-LC covalent dimers were secreted (**Fig. 2C**, lane 3), but HC-only secretion was not observed although the HC polypeptide was produced (**Fig. 2C**, lane 2). In the 7-day batch cell culture method used, the mAb-B secretion titer was ~26 mg/L on average (**Table 2**).

Based on the particulate morphology at neutral pH, we expected that mAb-B might induce needle-like inclusion bodies in the ER, but mAb-B induced classic RBs both at steady-state and upon cargo accumulation by BFA treatment. Under normal cell culture conditions, RB phenotype was observed in 13.5% of the transfected cells (**Fig. 2E**, first row; **Table 2**). Under the secretion block condition (**Fig. 2D**), the prevalence of RB phenotype cells increased to 40.0% (**Fig. 2E**, second and third rows; **Table 2**). For the HC-only and LC-only transfected cells, the RB phenotype frequency was 59.8% and 88.7%, respectively (**Fig. 2F**; **Table 2**). Similar to the case of mAb-A, BFA treatment markedly increased the number of RB-positive cells. Likewise, RB phenotype frequency was much higher when the subunit chains were expressed individually than when they were co-expressed.

RB phenotypes ensue from the overexpression of human IgG2κ mAb-C that readily induces irregular grain-like particles upon mechanical agitation stress

The third IgG clone, mAb-C, was distinguished by its high sensitivity to mechanical stress by agitation on an orbital shaker platform. Mechanical agitation of an antibody solution is believed to expose mAbs to unfolding stresses such as shear and air-liquid or surface-liquid interfaces.[23] Although this may not be a physiologically relevant stress, it is a key testing condition that mimics the process of biopharmaceutical shipping and transport in an accelerated manner and, as such, aims to identify physically unstable mAb clones.[23] When a concentrated mAb-C solution (70 mg/ml, at pH 5.0) was subjected to agitation stress for 72 hrs (see Materials and methods), the solution became clouded (**Fig. 3A**). When viewed with a DIC microscope, the post-agitation mAb-C solution was filled with irregular

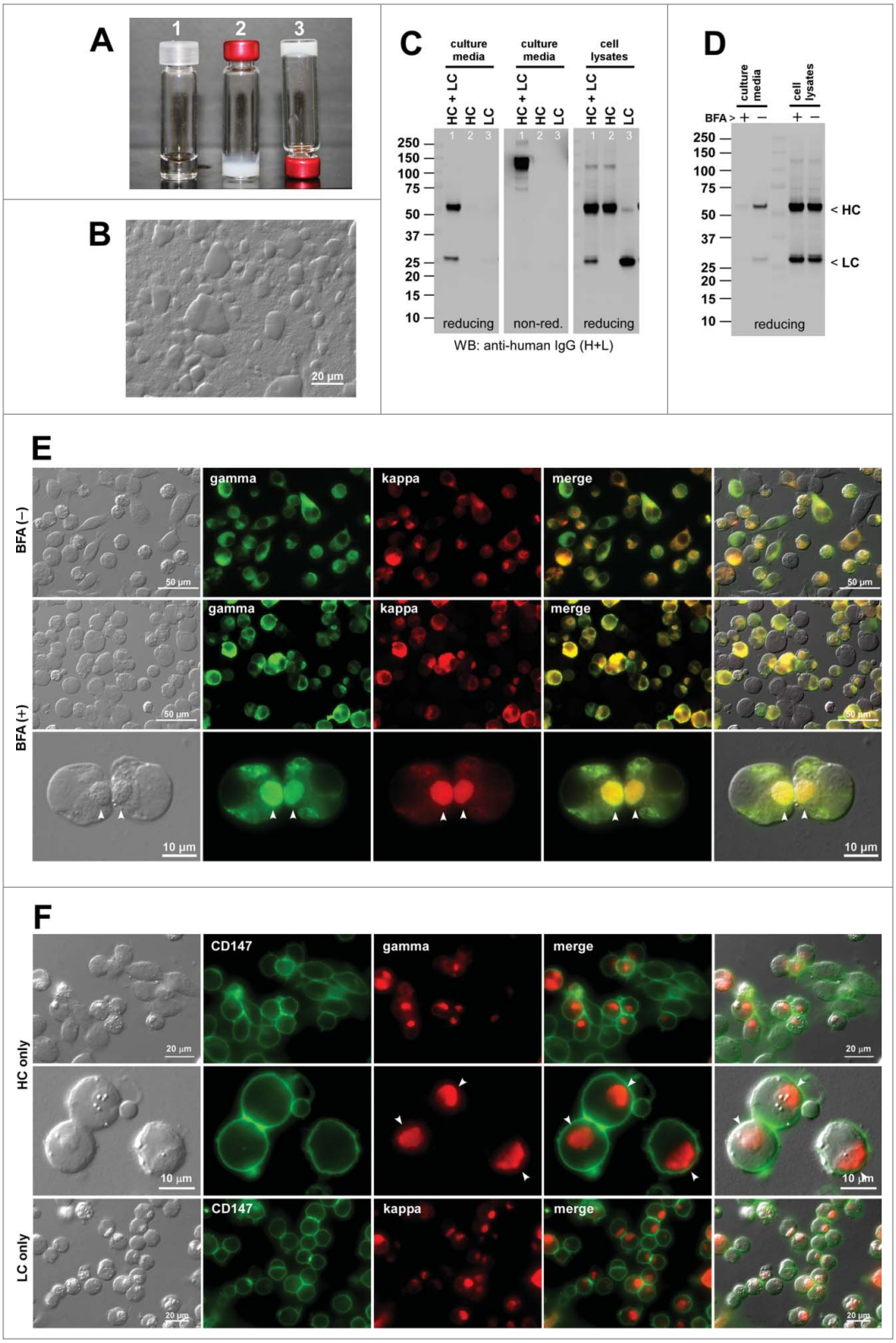

Figure 1. Human IgG2κ (mAb-A) forms gel at neutral pH environments in vitro and induces Russell bodies during biosynthesis. (**A**) Glass vials containing mAb-A solution at 70 mg/ml at pH 5.0 (vial 1) and at pH ~7.0 (vials 2 and 3). Vial-3 is placed upside down. (**B**) DIC micrograph of a gelated mAb-A solution. (**C**) Western blotting results for the cell culture media and cell lysates harvested on Day-7 post transfection. The expression constructs used are shown at the top of each lane. (**D**) Western blotting results on the cell culture media after 24 hr of BFA (15 μg/ml) or null treatment from Day-2 to Day-3 post transfection. The cell viabilities after the 24 hr BFA and mock treatment were 87.2% and 91.7%, respectively. (**E**) Fluorescent micrographs of HEK293 cells co-transfected with HC and LC constructs. Cells under null treatment are shown in the first row. Cells under BFA treatment are shown in the second and third rows. Green, anti-gamma staining. Red, anti-kappa staining. RBs are pointed by arrowheads in the bottom row. (**F**) Fluorescent micrographs of HEK293 cells transfected with HC construct (first 2 rows) or with LC construct (third row). Green, anti-CD147 staining. Red, anti-gamma or anti-kappa staining. Endogenous CD147 was stained to highlight cell surface and cell shape. RBs are pointed by arrowheads in the second row.

grain-shaped particulates (**Fig. 3B**). The particulate formation was effectively suppressed by adding 0.01% (w/v) Tween-20 to the mAb-C solution (data not shown). Beside the high agitation susceptibility, no other major issues were identified for mAb-C.

Co-transfection of HC and LC constructs into HEK293 cells resulted in the assembly and secretion of IgG (**Fig. 3C** left and right panels, lane 1). Because anti-human IgG polysera had different detection threshold, epitope coverage, and affinities to different subunit chains and isotypes, the Western blotting signal strengths did not always reflect the subunit stoichiometry. When individual subunit chains were transfected separately, the LC was

Table 2. Summary of secretion titers and phenotypes frequency. Secretion titers are shown in average ± standard deviation, followed by sample size in parentheses

mAb	Secretion titer (mg/L)	Cell phenotype at steady-state	Cell phenotype with Brefeldin A	Cell phenotype with thapsigargin	Cell phenotype HC only	Cell phenotype LC only
A	11.08 ± 4.85 (n = 5)	RB, 18.6% (85/457)	RB, 37.5% (192/512)	n.d.	RB, 65.8% (79/120)	RB, 90.6% (387/427)
B	26.38 ± 1.89 (n = 5)	RB, 13.5% (41/303)	RB, 40.0% (102/255)	n.d.	RB, 59.8% (113/189)	RB, 88.7% (407/459)
C	4.24 ± 2.71 (n = 9)	RB, 73.1% (517/707)	RB, 71.5% (402/562)	n.d.	RB, 65.2% (176/269)	RB, 77.4% (254/328)
D	27.31 ± 8.98 (n = 3)	RB, 58.7% (131/223)	RB, 58.8% (104/177)	n.d.	RB, 81.1% (154/190)	RB, 2.5% (4/157)
E	15.04 ± 7.98 (n = 7)	RB, 70.2% (643/916)	RB, 79.6% (422/530)	n.d.	RB, 34.1% (221/619)	RB, 96.7% (480/496)
F	64.48 ± 9.51 (n = 4)	RB or CB, 0% (0/353)	CB, 20.1% (85/422)	n.d.	Grape, 93.3% (404/433)	RB, 0.36% (1/274)
G	301.04 ± 51.47 (n = 8)	RB, 0.85% (2/234)	RB, 4.0% (9/224)	RB, 38.4% (87/226)	RB, 24.5% (5/232)	RB, 0.45% (1/218)

The type of phenotype is shown in abbreviations, followed by phenotype frequency (%) and the actual count number in parentheses. Abbreviations: RB, Russell body; CB, crystalline body; Grape, grape cell phenotype; n.d., not determined.

secreted in the form of monomers and covalently linked dimers (**Fig. 3C**, lane 3). The HC-only secretion, by contrast, was not observed despite the polypeptide being expressed (**Fig. 3C**, lane 2). The mAb-C secretion titer was ~4 mg/L on average (**Table 2**).

We explored what types of cellular phenotypes were induced by the expression of this agitation-sensitive mAb-C. At steady state conditions, RB phenotype was induced in 73.1% of the transfected cells (**Fig. 3E**, first 2 rows; **Table 2**). Under the 24-hr BFA treatment conditions that block IgG secretion (**Fig. 3D**), the frequency of the RB-positive cells remained about the same (71.5%; **Fig. 3E**, third row; **Table 2**). The frequency of RB phenotypes for the HC-only and LC-only transfected cells was 65.2% and 77.4%, respectively (**Fig. 3F**; **Table 2**).

Induction of RB phenotypes by the overexpression of agitation-sensitive human IgG2κ mAb-D

The fourth model IgG clone, mAb-D, was also known for its high susceptibility to a mechanical agitation stress. When mAb-D solution was subjected to agitation for 72 hrs, the solution became turbid (**Fig. 4A**). Unlike that of mAb-C, generated microscopic particulates were amorphous (**Fig. 4B**). Beside the high agitation susceptibility, no other major issues were found.

Co-expression of HC and LC led to the assembly and the secretion of IgG (**Fig. 4C**, lane 1). In the 7-day cell culture method, the mAb-D secretion titer was ~27 mg/L on average (**Table 2**). The LC-only expression resulted in an abundant secretion of LC both in monomers and disulfide-linked dimers (**Fig. 4C**, lane 3). The HC-only construct was not secreted despite the protein synthesis (**Fig. 4C**, lane 2).

Both at steady-state and under BFA treatment (**Fig. 4D**), roughly 59% of the transfected cells induced RB phenotypes (**Fig. 4E**; **Table 2**). The frequency of RB phenotypes for the HC-only expression was 81.1% (**Fig. 4F**, top; **Table 2**). The LC-only transfection, by contrast, induced RB phenotypes only in 2.5% of the transfected cells (**Fig. 4F**, bottom; **Table 2**) and partly accounted for why the LC-only secretion was so abundant. In contrast to the 2 mAb clones with solubility issues at neutral pH (see Sections 2.1 and 2.2 above), the frequency of RB-positive cells did not increase by blocking the ER-to-Golgi transport for the 2 agitation-susceptible mAb clones.

RB phenotypes are induced by the human IgG2κ mAb-E that causes unusually high solution viscosity

The fifth IgG clone, mAb-E, had no major issues in mechanical stress and solubility at neutral pH, yet it was deemed undesirable as a therapeutic lead candidate because of its unusually high solution viscosity. Within a range of tested concentrations from 70 mg/ml to 145 mg/ml, the viscosity of the mAb-E solution was much higher than that of mAb-C, which largely fell within an expected range for a mAb in this testing condition (**Fig. 5A**). To meet efficacious dosing requirements and subcutaneous administration volume limits, antibody therapeutics are often concentrated to >100 mg/ml in aqueous solution. High viscosity of mAb solution therefore poses a problem in drug administration by injection.[24] Furthermore, the overproduction of highly viscous mAb clones in vivo is likely to exacerbate the pathogenesis of hyperviscosity syndromes associated with hypergammaglobulinemia and multiple myeloma.[25]

Co-expression of HC and LC resulted in the secretion of assembled mAb-E (**Fig. 5B**, lane 1). Similar to many other mAbs, the LC-only expression led to the secretion of LCs (**Fig. 5B**, lane 3). A modest level of HC-only secretion was also observed (**Fig. 5B**, lane 2). The secreted HC-only species was covalently aggregated into high molecular weight species when analyzed under non-reducing conditions (data not shown). The mAb-E secretion titer was ~15 mg/L on average (**Table 2**).

At steady state and under the effective BFA dosing (**Fig. 5C**), 70.2% and 79.6% of the transfected cells induced RB phenotypes, respectively (**Fig. 5D**; **Table 2**). The frequency of RB phenotypes for the HC-only expression was 34.1% (**Fig. 5E**; **Table 2**). The LC-only transfection, on the other hand, induced RB phenotypes extensively in 96.7% of transfected cells (**Fig. 5F**; **Table 2**).

Crystalline body phenotype is induced by a human IgG2κ mAb-F that readily crystallizes at neutral pH

As a reference mAb, we re-visited the human IgG2κ clone that was recently characterized and shown to possess high

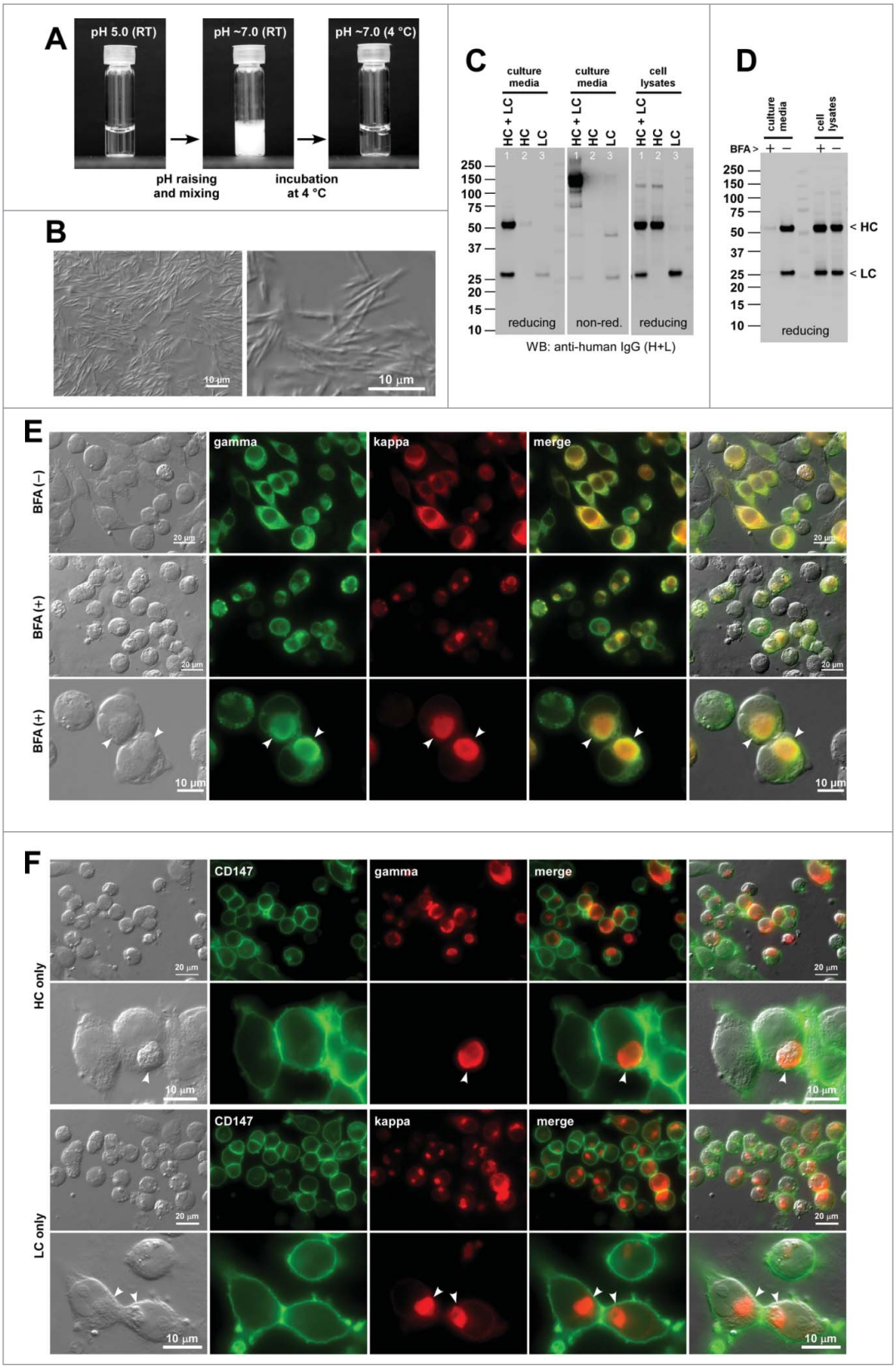

Figure 2. Human IgG2κ (mAb-B) forms needle-shaped aggregates at neutral pH in vitro and induces Russell bodies in the ER. (**A**) Glass vial containing mAb-B solution at 70 mg/ml at pH 5.0 (left) and after pH shift to pH ~7.0 followed by a brief mixing (middle). The vial shown in the middle panel was subsequently kept at 4°C for 24 hr (right). (**B**) DIC micrographs of the clouded mAb-B solution after pH raising. (**C**) Western blotting results for the cell culture media and cell lysates harvested on Day-7 post transfection. The expression constructs used for transfection are shown at the top of each lane. (**D**) Western blotting results on the cell culture media and cell lysates after 24 hr of BFA or null treatment from Day-2 to Day-3 post transfection. The cell viabilities after the 24 hr BFA and mock treatment were 94.6% and 96.9%, respectively. (**E**) Fluorescent micrographs of HEK293 cells co-transfected with HC and LC constructs. Cells at steady-state are shown in the first row. Cells under BFA treatment are shown in the second and third rows. Green, anti-gamma staining. Red, anti-kappa staining. RBs are pointed by arrowheads in the bottom row. (**F**) Fluorescent micrographs of HEK293 cells transfected with HC construct (first 2 rows) or with LC construct (bottom 2 rows). Green, anti-CD147 staining. Red, anti-gamma or anti-kappa staining. RBs are pointed by arrowheads in the second and fourth rows.

crystallization propensity at neutral pH, both in vitro and in the ER.[19] The solubility of mAb-F was high in an acidic environment at 70 mg/ml (**Fig. 6A-1**). However, mAb-F readily crystallized (i.e., went through liquid-solid phase separation) upon shifting the solution pH to a neutral range and instantly sedimented to the bottom (**Fig. 6A-2**). The precipitates were composed of rod- and bullet-shaped crystalline materials (**Fig. 6B**).

Co-transfection of HC and LC resulted in a robust secretion of fully assembled IgG (**Fig. 1C**, lane 1). When individual

subunit chains were independently expressed, the LC was abundantly secreted as monomers and covalent dimers (**Fig. 6C**, lane 3). The HC was not secreted to the culture media despite the HC polypeptide expression (**Fig. 6C**, lane 2). The mAb-F secretion titer was ~64 mg/L on average using the 7-day cell culture method (**Table 2**).

Under normal cell growth conditions, mAb-F expressing cells did not induce any inclusion body phenotypes (**Fig. 6E**, first row; **Table 2**). When the protein secretion was blocked for 24 hrs by BFA treatment (**Fig. 6D**), 20.1% of the transfected cells induced rod-shaped crystalline bodies (CBs) (**Fig. 6E**, second and third rows; **Table 2**), but no RB was observed. Unlike RBs that can be directly stained by anti-gamma and anti-kappa, the rod-shaped CBs were not stained by the same set of antibodies due to their crystalline nature that prevents the penetration of staining antisera. For the HC-only transfected cells, a variant of RB so-called "grape cell" phenotype[26] was induced in 93.3% of the HC-expressing cells (**Fig. 6F**, first 2 rows; **Table 2**). Less than 1% of the LC-only transfected cells induced RB phenotype (0.36%; **Fig. 6F**, bottom row; **Table 2**). The co-expression of HC and LC subunits were required for CB phenotype induction, but importantly such propensities were not predictable from the phenotypes induced by the expression of individual subunits.

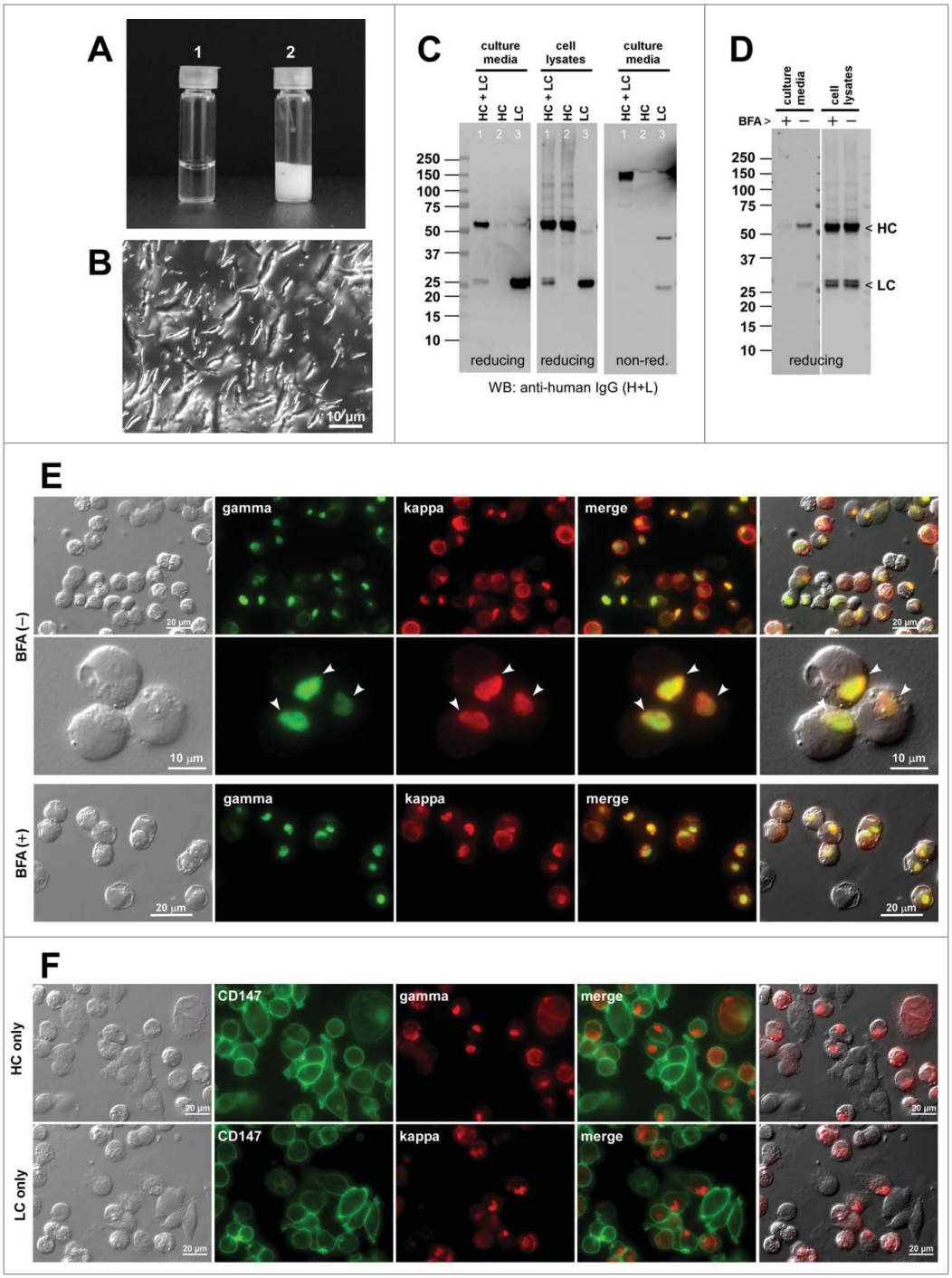

Figure 3. Agitation-sensitive human IgG2κ (mAb-C) induces Russell body phenotype. (**A**) Glass vials containing mAb-C solution at 70 mg/ml at pH 5.0 at room temperature before (left) and after (right) the subjection to agitation stress. The actual stress was applied in a 3-ml vial (see Materials and Methods). The content was transferred to a 1-ml vial before the photograph was taken. (**B**) DIC micrograph of the clouded mAb-C solution after the agitation stress. (**C**) Western blotting results for the cell culture media and cell lysates harvested on Day-7 post transfection. The used expression constructs are shown at the top of each lane. (**D**) Western blotting results on the cell culture media and cell lysates after 24 hr of BFA or null treatment from Day-2 to Day-3 post transfection. The cell viabilities after the 24 hr BFA and mock treatment were 84.6% and 88.3%, respectively. (**E**) Fluorescent micrographs of HEK293 cells co-transfected with HC and LC constructs. Cells at steady state are shown in the first 2 rows. Cells under BFA treatment are shown in the third row. Green, anti-gamma staining. Red, anti-kappa staining. RBs are pointed by arrowheads in the bottom row. (**F**) Fluorescent micrographs of HEK293 cells transfected with HC construct (first row) or with LC construct (second row). Green, anti-CD147 staining. Red, anti-gamma or anti-kappa staining.

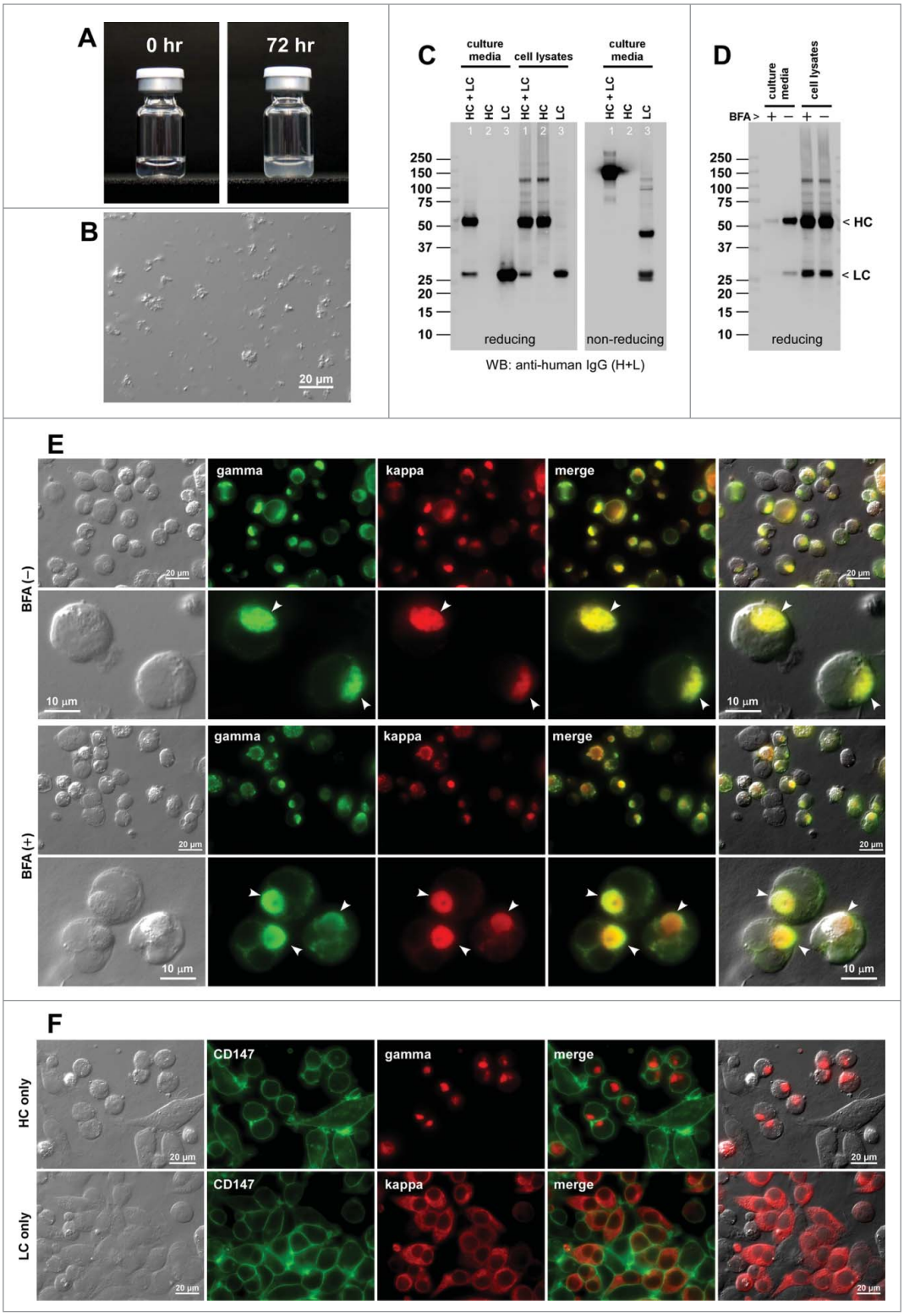

Figure 4. Agitation sensitive human IgG2κ (mAb-D) induces Russell body during immunoglobulin biosynthesis. (**A**) Glass vials containing mAb-C solution at 70 mg/ml at pH 5.0 at room temperature at 0 hr (left) and after 72 hr agitation stress (right). (**B**) DIC micrograph of a mAb-D solution after the agitation stress. (**C**) Western blotting results for the cell culture media and cell lysates harvested on Day-7 post transfection. The transfected expression constructs used for transfection are shown at the top of each lane. (**D**) Western blotting results on the cell culture media and cell lysates after 24 hr of BFA or null treatment from Day-2 to Day-3 post transfection. The cell viabilities after the 24 hr BFA and mock treatment were 85.0% and 88.0%, respectively. (**E**) Fluorescent micrographs of HEK293 cells co-transfected with HC and LC constructs. Cells at steady-state are shown in the first 2 rows. Cells under BFA treatment condition are shown in the third and fourth rows. Green, anti-gamma staining. Red, anti-kappa staining. RBs are pointed by arrowheads in the second and fourth rows. (**F**) Fluorescent micrographs of HEK293 cells transfected with HC construct (first row) or with LC construct (second row). Green, anti-CD147 staining. Red, anti-gamma or anti-kappa staining.

Cellular phenotypes induced by the overexpression of human IgG1κ mAb-G that shows no major solubility issues in vitro

Not all human IgG mAb clones have the propensity to induce RB or CB phenotypes under the same expression conditions. One such example is mAb-G. Although absence of evidence is not evidence of absence, no notable solution behavior issues were associated with mAb-G (unpublished data).

Co-transfection of HC and LC resulted in an abundant secretion of fully assembled IgG (**Fig. 7A**, lane 1).

When the LC subunit was independently expressed, a high level LC secretion was observed as monomers and disulfide-linked dimers (**Fig. 7A**, lane 3). The HC-only secretion was also

marginally detectable (**Fig. 7A**, lane 2). The mAb-G secretion titer was ~300 mg/L on average (**Table 2**), and was at the high end of secretion output range in this batch cell culture system.

When cellular phenotypes were examined during mAb-G overexpression, less than 1% of the transfected cells exhibited RB phenotypes at steady-state conditions (**Fig. 7B**, lane 1; **Fig. 7C**, top row, **Table 2**). Even when the secretion was blocked by BFA treatment (**Fig. 7B**, lane 2), RB phenotypes were induced in no more than 4.0% of the transfected cells (**Fig. 7C**, second row; **Table 2**). To gauge the degree of intrinsic protein solubility in intracellular environments, we tested whether mAb-G expressing cells can withstand an adverse cell culture condition without inducing RB phenotypes. To this end, we treated the cells with thapsigargin to deplete free calcium from the ER lumen and to disrupt ER resident proteins functions. Similar to what was shown previously for a different set of high-secreting IgG clones,[15] thapsigargin treatment was effective in inducing RB-like phenotypes in 38.4% of the transfected cells (**Fig. 7B**, lane 3; **Fig. 7C**, bottom; **Table 2**). This suggested that even an IgG mAb clone with no major

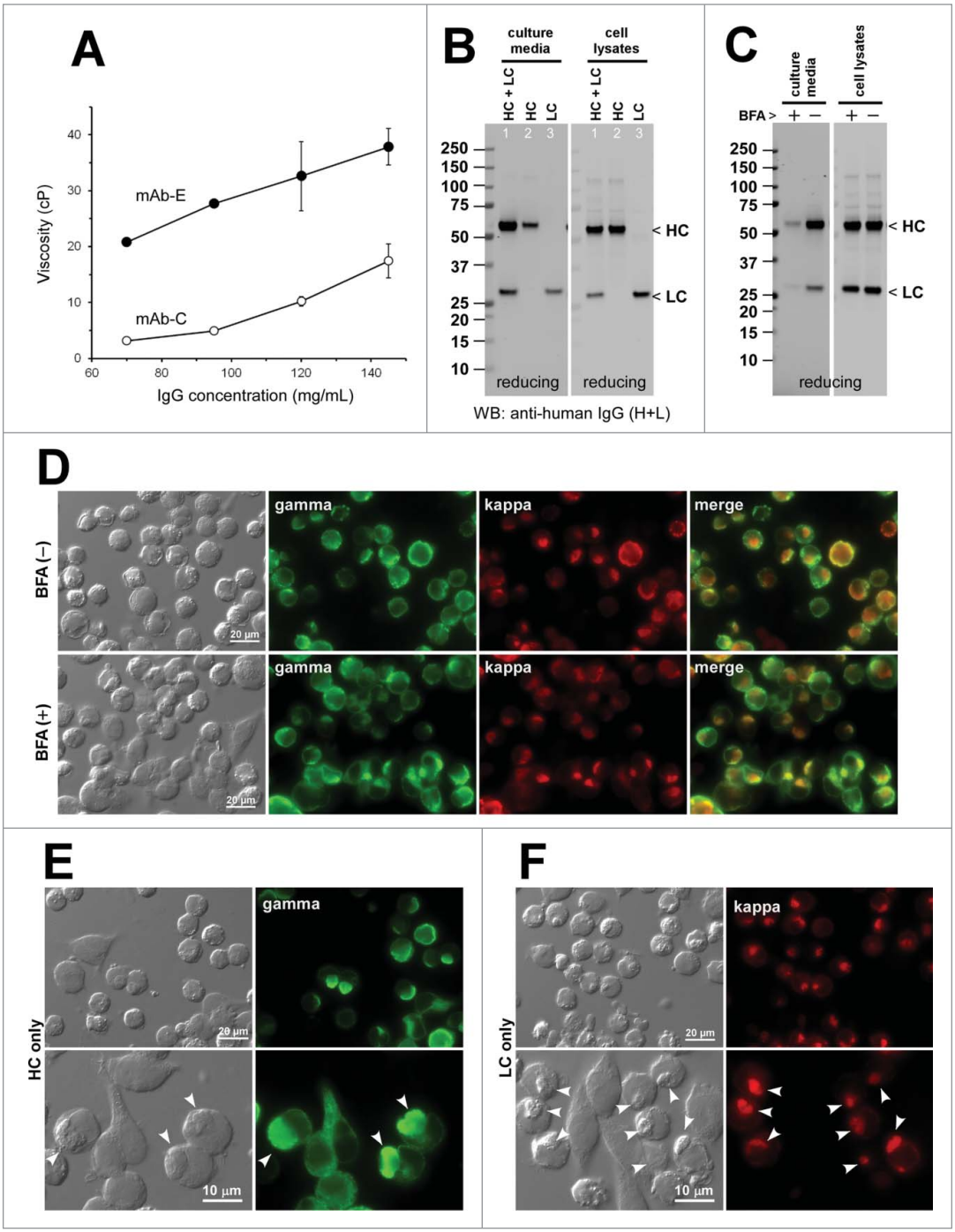

Figure 5. High viscosity-causing human IgG2κ mAb-(E)induces Russell body phenotypes. (**A**) Viscosity of mAb-E solution (closed circle) and mAb-C solution (open circle) was measured at 70, 95, 120, and 145 mg/ml in triplicate. Error bars denote standard deviation. Centipoise (cP) is a dynamic viscosity measurement unit. (**B**) Western blotting results for the cell culture media and cell lysates harvested on Day-7 post transfection. The expression constructs used for transfection are shown at the top of each lane. (**C**) Western blotting results on the cell culture media and cell lysates after 24 hr of BFA or null treatment from Day-2 to Day-3 post transfection. The cell viabilities after the 24 hr BFA and mock treatment were 85.2% and 89.8%, respectively. (**D**) Fluorescent micrographs of HEK293 cells co-transfected with HC and LC constructs. Cells at steady state are shown in the first row. Cells under BFA treatment condition are shown in the second row. Green, anti-gamma staining. Red, anti-kappa staining. (**E and F**) Fluorescent micrographs of HEK293 cells transfected with HC construct, shown in green (**E**) or with LC construct, shown in red (**F**). RBs are pointed by arrowheads in the bottom row.

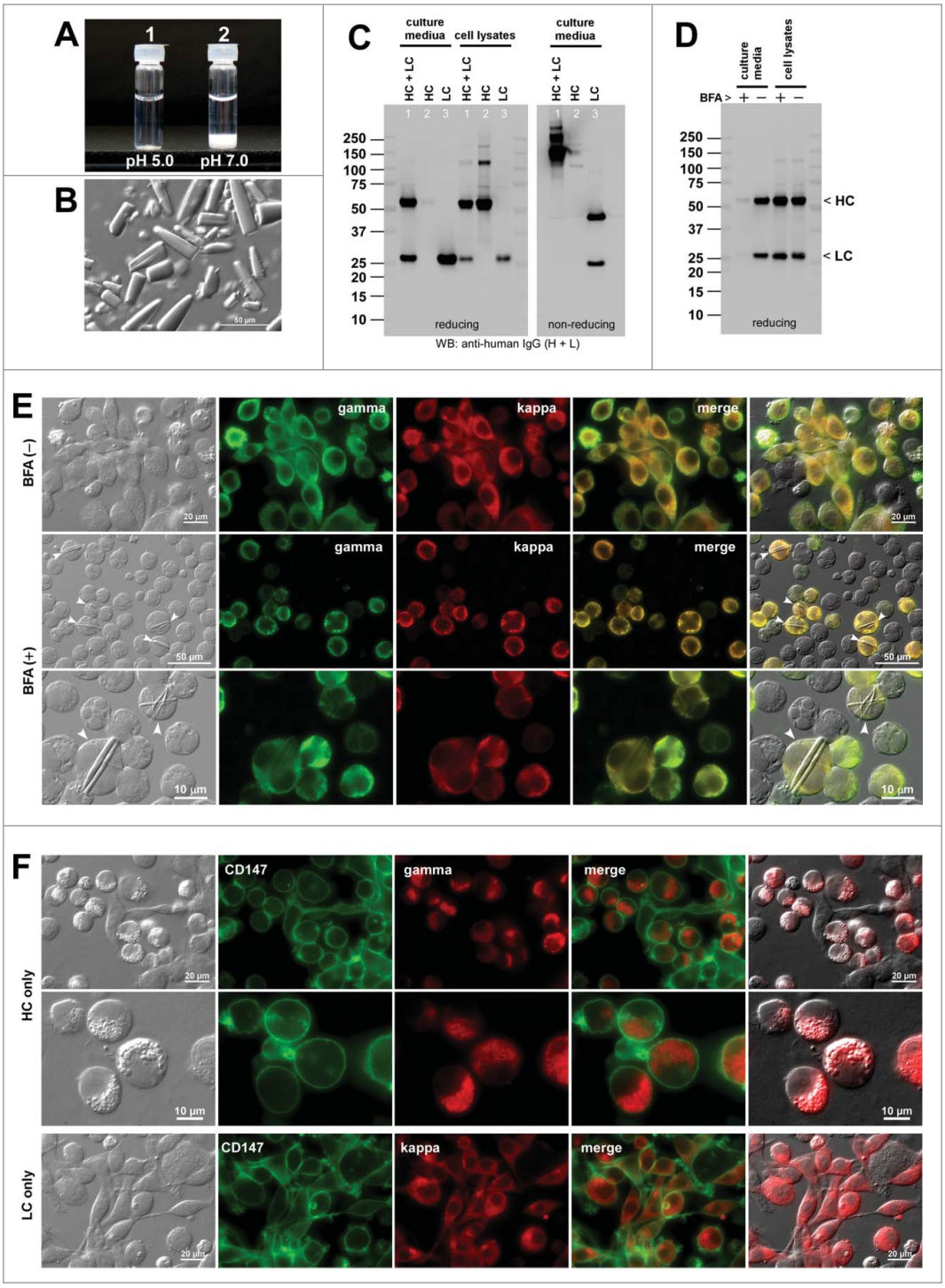

Figure 6. Human IgG2κ mAb-F readily crystallizes at neutral pH both in vitro and in the ER. (**A**) Glass vial containing 70 mg/ml mAb-F solution at pH 5.0 (left) and after pH shift to pH ~7.0 (right). (**B**) DIC micrograph of the precipitated materials recovered from the bottom of vial-2. (**C**) Western blotting results for the cell culture media and cell lysates harvested on Day-7 post transfection. The expression constructs used for transfection are shown at the top of each lane. (**D**) Western blotting results on the cell culture media after 24 hr period of BFA or null treatment from Day-2 to Day-3 post transfection. The cell viabilities after the 24 hr BFA and mock treatment were 93.3% and 95.4%, respectively. (**E**) Fluorescent micrographs of HEK293 cells co-transfected with HC and LC constructs. Cells under null treatment are shown in the first row. Cells under BFA treatment are shown in the second and third rows. Cells containing readily identifiable crystalline bodies are marked by arrowheads. Green, anti-gamma staining. Red, anti-kappa staining. (**F**) Fluorescent micrographs of HEK293 cells transfected with HC construct (top 2 rows) or with LC construct (third row). Green, anti-CD147 staining. Red, anti-gamma or anti-kappa staining.

solubility issues in vitro can still aggregate into RBs during biosynthesis if the functions of ER resident proteins were perturbed. Despite the apparent disruption of normal ER functions, mAb-G was nonetheless secreted during the 24-hr thapsigargin treatment, albeit at a lower level (**Fig. 7B**, lane 3). The frequency of RB phenotypes for the HC-only expression was 24.5% (**Fig. 7D**, top; **Table 2**). The LC-only transfection induced RB phenotypes in 0.45% of transfected cells (**Fig. 7D**, bottom; **Table 2**).

Discussion

How precisely will intracellular biosynthetic events predict the extracellular solution behaviors of an IgG mAb clone?

Tangible explanations on why some full-length human IgG clones induce RB formation much more readily than others have been elusive. It has also been a puzzle as to why the secretion output of some IgG clones is much lower than others. Whether those events are related and are of physiological importance have not been addressed to date. We tackled these problems by examining a panel of model IgG mAb clones for which we know the detailed molecular attributes in advance. This approach not only uncovered important clues to what types of full-length IgGs can preferentially induce RB phenotypes during biosynthesis, but also

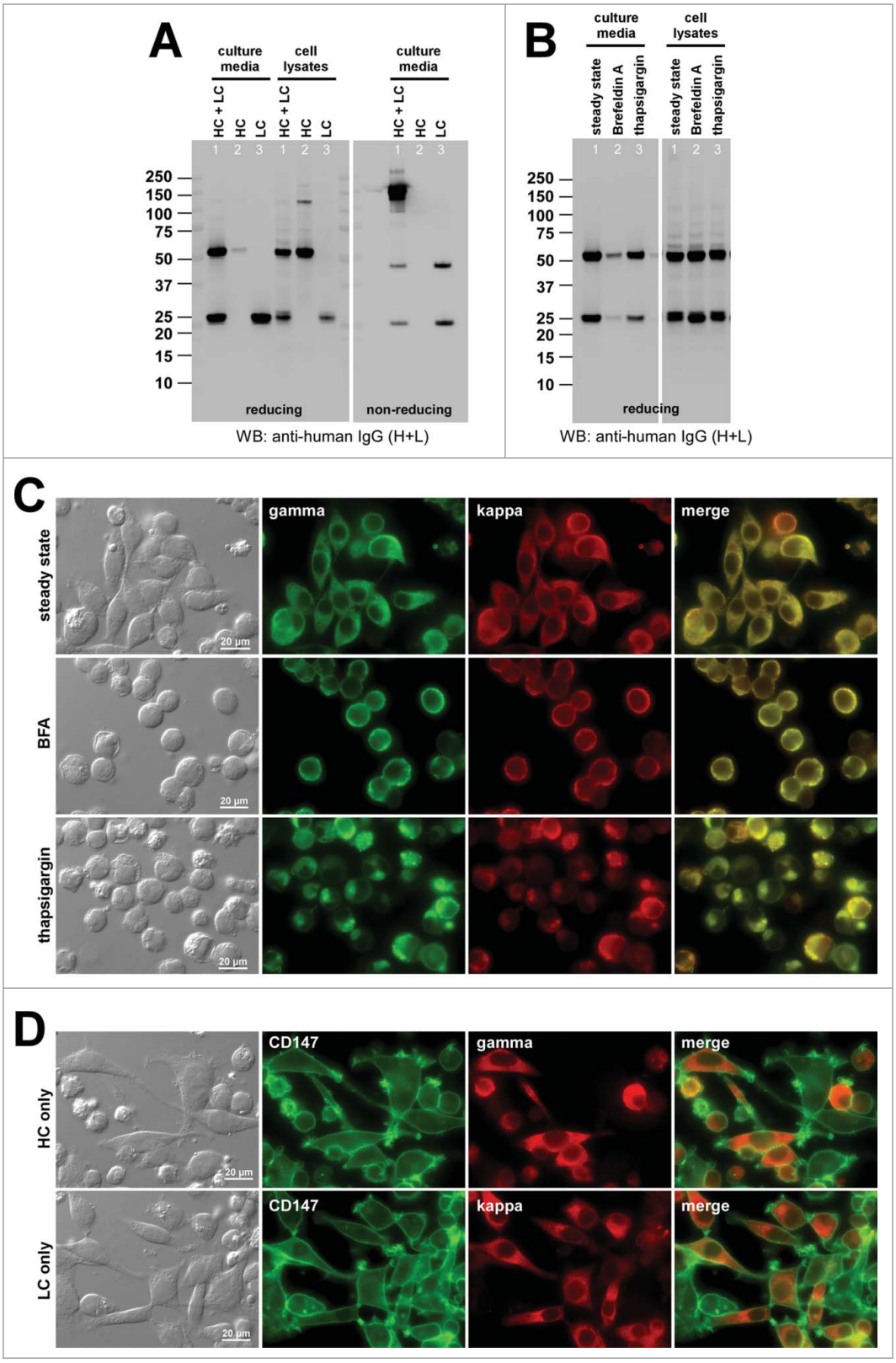

Figure 7. Cellular phenotypes induced by the high-secreting human IgG1κ mAb-G under different cell culture conditions. (**A**) Western blotting results for the cell culture media and cell lysates harvested on Day-7 post transfection. The expression constructs used are shown at the top of each lane. (**B**) Western blotting results on the cell culture media and cell lysates after 24 hr of null (lane 1), 15 μg/ml BFA (lane 2), or 1 μM thapsigargin (lane 3) treatment from Day-2 to Day-3 post transfection. The cell viabilities after the 24 hr BFA, thapsigargin, and mock treatment were 82.0%, 84.2%, and 85.2%, respectively. (**C**) Fluorescent micrographs of HEK293 cells co-transfected with HC and LC constructs. Cells under null treatment are shown in the first row. Cells under BFA and thapsigargin treatment are shown in the second and third row, respectively. Green, anti-gamma staining. Red, anti-kappa staining. (**D**) Fluorescent micrographs of HEK293 cells transfected with HC construct (top row) or with LC construct (bottom row). Green, anti-CD147 staining. Red, anti-gamma or anti-kappa staining.

provided physiological contexts to the enigmatic RB phenotype induction. Five model mAb clones exhibiting 'unfavorable' solution behaviors induced RB phenotypes during immunoglobulin biosynthesis at steady state and under a pharmacological block of ER-to-Golgi transport. Another IgG mAb clone that readily crystallized at neutral pH in vitro also induced crystal formation in the neutral pH environment of the ER lumen. Conversely, one representative IgG mAb clone with no notable solution behaviors did not induce RB-like phenotypes unless the ER functions were severely compromised by thapsigargin treatments. These observations led us to think that predisposed high aggregation propensities (associated with a subset of IgG clones) affect the fate of an antibody molecule from the beginning of its protein life, still being synthesized in the ER and before transported out of the ER. The RB (and CB) induction could thus be the earliest first-hand evidence by which we can distinguish intrinsically aggregation-prone IgG mAb clones from innocuous

generic mAb clones. Because imaging assays are amenable to high throughput formats, phenotype screening of IgG-expressing cells has the potential to become a tool for identifying and disqualifying undesirable IgG clones from the lead candidate pool at the early stage of an antibody drug discovery program.

Does the HC isotype play roles in providing distinct properties to immunoglobulins? In our testing mAb panel, the innocuous mAb happened to be IgG1κ and all the mAbs with solution behavior issues were IgG2κ. Is this observation generalizable? There is a suggestion that, on average, IgG2s are more aggregation-prone than IgG1s in vitro.[27] When it comes to the biosynthesis, however, Stoops et al. reported that G1 to G2 isotype switching did not affect the RB-inducing propensities and the secretion titers of 3 independent human IgG clones.[15] In clinical settings, RB formation is observed for other HC classes such as IgA and IgM.[6] Likewise, in immunoglobulin deposition diseases, disease-causing immunoglobulins are not restricted to IgG2.[6] For those immunoglobulins that can induce CB phenotypes, the HC isotype differences appeared to modulate biosynthetic processes in cellulo.[22,28] Overall, a consistent guiding model is still missing for the roles of HC isotypes on immunoglobulin's properties in vitro, in cellulo, and in vivo. Furthermore, uncovering the rules for certain structural features (either linear or conformational) that would contribute to IgG crystallization or phase separation phenomena require further investigation.

Why does BFA treatment exacerbate the RB phenotypes when the mAbs possess low solubility issues at neutral pH, but not so much in other cases? One likely scenario is that BFA treatment temporarily elevated the concentration of export ready IgG species in the ER lumen and helped reach the solubility limit more readily when the IgG clone in question had inherent solubility problems at neutral pH environment. The neutral pH of the ER lumen likely played a role in such event. Similar principles should also apply to the CB phenotype induction.[19,22]

Because the 2 compared environments (i.e., in the ER lumen and in test tube) are fundamentally different, identical phenotypic responses may not always occur between the cell imaging assays and in vitro assays. For example, folding intermediates and the resident proteins co-exist in a highly crowded environment of the ER, yet the chemical composition of the ER lumen is not precisely understood except the pH being neutral.[29] By contrast, in a test tube setting, purified IgG mAbs are usually the only protein constituent in a chemically defined buffer solution. Whereas neither can exact IgG concentration in the ER be measured in each cell nor normalized among transfected cells, the concentration of IgG can be set at will in test tubes. Moreover, different types of aggregation propensities and condensation events are usually identified under different conditions using dedicated in vitro assays designed to measure specific attributes of interest. It could therefore be difficult for a cell imaging assay to be able to fully distinguish such diverse IgG condensation events. In a cellular setting, different types of solution behaviors will be represented by a limited number of phenotypic readouts, with varying frequency, morphology, or response to pharmacological treatments.

Finding a shared cellular phenotype during the overexpression of 5 poorly-behaved IgG mAb clones does not instantly mean that all poorly behaving IgG mAb clones would induce RB phenotypes during biosynthetic steps although it is an attractive possibility. Whether all IgG clones with pronounced solution behaviors would preferentially induce RBs is difficult to test because we usually do not have resources to examine the entire clonal repertoires. Similarly, for the IgG mAb clones that do not induce RB phenotypes, it would be difficult to prove that they have no solution behavior issues outside of the assay conditions used. Likewise, the question of assay linearity across multiple parameters is difficult to address in a controlled manner because such an experiment would require a series of closely related IgG mAb clones with varying degrees of severity for a given solution behavior of interest. The strongest type of evidence that could support our view would be the genetic one in which a point mutation rectifies the unfavorable solution behaviors in vitro and concurrently eliminates RB phenotypes during biosynthesis. Such mutants were identified previously for the crystallizing mAb-F,[19] but we have not found such variants for the 5 RB-inducing IgG mAbs used here.

Implications for the physiological roles of Russell body formation in vivo

The prevailing view of the RB formation is that it is an ER protein control mechanism that prevents the secretion of abnormally truncated or deleted immunoglobulin proteins.[17,18] This hypothesis was derived from the studies using a secretion-incompetent mutant of mouse μ-HCs lacking the CH1 domain.[17,18] Based on the cell phenotype similarities to the ER storage diseases caused by a group of mutant proteins,[30] a possible involvement of RBs in the pathogenesis of such disease process was considered.[17] While this interpretation remains attractive, it does not address the issue of pre-existing differences in RB-inducing propensities among functional (and secretion-competent) human IgG clones with no gross sequence abnormalities.[15] Based on the insights from this study, we propose that RB induction represents a phase separation event taking place in the ER lumen or a loss of colloidal stability of the overexpressed IgG mAb in the physiological environment of the ER. This model predicts that the IgG mAb clones with intrinsically high condensation/aggregation propensities would preferentially reach the RB-inducing threshold in the ER lumen. Intrinsic physicochemical properties of the cargo therefore play critical roles in determining the secretion output potential by directly affecting the biosynthetic steps. As such, RB formation could serve as a mechanism to limit the release of (thus the serum concentration of) immunoglobulins with high aggregation/condensation properties and preemptively reduce the risk of immunoglobulin deposition diseases.

Various roles and explanations have been proposed for the enigmatic RBs during the last 120 years. William Russell originally asserted that RB was a parasitic intracellular fungus that causes cancer.[31] This hypothesis was not well supported, obviously, and this view is revisited mostly for a historical reason. Our study offered a new role for RBs as a potential cellular mechanism to restrict the secretion of intrinsically aggregation-prone (thus potentially harmful and pathogenic) IgG mAb clones to the extracellular space. To strengthen this view, examination of

the biosynthetic steps for the *bona fide* pathogenic immunoglobulin clones derived from the patients of immunoglobulin deposition diseases would be valuable.

Material and Methods

Chemicals, detection antibodies, and human IgG mAbs

All the chemicals, bioactive compounds, and reagents were obtained from Sigma-Aldrich. FITC-labeled mouse anti-CD147 was from BD Transduction Laboratories. Affinity purified Rabbit polyclonal anti-human IgG (H+L) antibody was from Jackson ImmunoResearch Laboratories. FITC-conjugated goat anti-human gamma and Texas Red-conjugated goat anti-human kappa antibodies were from Southern Biotech. Seven recombinant human IgG mAb proteins (mAb-A, -B, -C, -D, -E, -F, -G) used for in vitro assays were obtained from Amgen's purified protein repository. In brief, the mAbs were produced using stably transfected proprietary Chinese hamster ovary cell lines developed in Amgen Inc. Human mAbs were then purified from the culture media by Protein-A affinity chromatography followed by cation exchange chromatography in order to achieve >95% homogeneity.

Expression constructs

The coding sequences for LC and HC were obtained from Xenomouse™-derived cognate hybridoma cell lines by using the molecular cloning method described previously.[15] Recombinant sequences of interest, either cloned from hybridoma or excised from pre-existing stable expression vectors, were subcloned into a pTT5 expression vector (obtained from National Research Council of Canada) by commonly used molecular cloning techniques. The germline gene segment usage for the VH and VL sequences was analyzed by using VBASE.[32]

HEK293 cell culture and transient transfection

HEK293-EBNA1 cells were obtained from National Research Council of Canada and were cultured in a humidified incubator (37°C, 5% CO_2) using Freestyle 293 media (Life Technologies). To grow cells in suspension format, the cells were cultivated in shaker flasks (Corning) placed on an Innova 2100 platform (New Brunswick Scientific). Expression constructs were transfected into HEK293 cells using the protocols detailed elsewhere.[15] A cognate pair of HC and LC constructs was co-transfected at one-to-one plasmid DNA mass ratio. When individual HC or LC constructs were transfected separately, one-half of the total DNA was substituted by an empty vector to normalize recombinant gene dosage. At 24-hr post transfection, cells were supplemented with Difco yeastolate (BD Biosciences). Cell culture media and whole cell lysates were collected on Day-7 post transfection. The concentration of secreted IgG in the harvested culture media was determined with an Octet RED96 (ForteBio) using Protein-A biosensors. To assess the effect of Brefeldin A (BFA) treatment on protein secretion, growth media of HEK293 suspension cell culture were replaced with fresh media with or without 15 μg/ml of BFA at 48 hrs post transfection. The cells were kept in suspension format for another 24 hrs before the culture media and cell lysates were harvested and analyzed by Western blotting.

SDS-PAGE and Western blotting

NuPAGE 4–12% Bis-Tris gradient gel and the accompanying buffer system (both from Life Technologies) were used to perform SDS-PAGE. Centrifugation-harvested cell pellets were directly lysed in SDS sample buffer (Life Technologies) and heated for 5 min at 90°C. Likewise, harvested cell culture media were mixed with SDS sample buffer and heat treated. For protein analysis under reducing conditions, 5% (v/v) β-mercaptoethanol was added to the sample buffer. For non-reducing analysis, 2 mM N-ethylmaleimide was included as an alkylating agent. Whole cell lysates corresponding to 12,000–12,500 cells were analyzed per lane. To compare the differences in volumetric secretion levels, equal volume (5 μl) of harvested cell culture media was analyzed per lane. Resolved proteins were electrotransferred to a nitrocellulose membrane, blocked with fluorescent Western blocking buffer (Rockland Immunochemicals), and probed with rabbit polysera against human IgG (H+L) obtained from Jackson ImmunoResearch Laboratories. After washes in PBS containing 0.05% (v/v) Tween-20, the nitrocellulose membranes were probed with AlexaFluor 680-conjugated secondary antibodies (Life Technologies). The fluorescent Western images were acquired using an Odyssey® infrared imaging system available from LI-COR Biosciences.

Immunofluorescent microscopy

At 48 hrs post transfection, growth media of HEK293 suspension cell culture were replaced with fresh media with or without 15 μg/ml of BFA. HEK293 cells (one million cells per well) were then seeded to poly-L-lysine coated glass coverslips placed in a 6-well plate and quiescently cultured for 24 hrs. The cells were fixed in 100 mM sodium phosphate, pH 7.2, containing 4% (w/v) paraformaldehyde for 30 min at room temperature. After washing steps in PBS containing 100 mM glycine, the fixed cells were incubated with permeabilization buffer (PBS containing 0.4% (w/v) saponin, 1% (w/v) BSA, 5% (w/v) fish gelatin) for 15 min, followed by incubation with FITC- or Texas Red-conjugated anti-gamma chain, anti-kappa chain, or anti-CD147 antibodies for 60 min. After washes in permeabilization buffer, coverslips were mounted to glass slides using Vectashield mounting media (Vector Labs). The slides were analyzed using a Nikon Eclipse Ti-E microscope with a 100×, 60×, or 40× CFI Plan Apocromat oil objective lens and Chroma FITC-HYQ or Texas Red-HYQ filter. Images were acquired using a Cool SNAP HQ2 CCD camera (Photometrics) and Nikon Elements imaging software. To determine Russell body (RB) or crystalline body (CB) phenotype frequencies, microscopic images of 10–50 randomly chosen fields were captured for each construct set using 60× objective lens. Based on the anti-gamma and anti-kappa co-staining, the total number of transfected cells was first determined for each condition. The presence of RB or CB phenotypes was determined by visual inspection in order to calculate the prevalence of phenotype-positive cells.

Antibody solution pH shift

After Protein-A purification, testing human IgG mAbs were concentrated to 70 mg/ml using 10,000 MWCO Amicon Ultra-15 (Millipore) in 10 mM acetate-buffered (pH 5.0) isotonic sucrose solution (hereafter mAb buffer). The concentrated mAb solution (100, 300, or 500 μl) was dispensed into a 1-ml glass vial and equilibrated to room temperature. To facilitate a pH shift to a neutral range, one-twentieth volume of 20× PBS (pH 7.4) was added to the glass vial, mixed briefly, and kept at room temperature for one hour. Glass vials were photographed and the mAb solutions were examined with a DIC microscope.

Mechanical agitation of mAb solution

After concentrating to 70 mg/ml in mAb buffer, 500 μl of testing mAb solution was dispensed into 3-ml glass vials. The vials were then placed in an upright position onto a foam-lined vial holder affixed to an orbital shaker (VWR, model OS-500; orbital diameter, 19 mm). The mAb solutions were mechanically agitated at 500 rpm for 72 hrs at ambient temperature in the dark. Glass vials were photographed, and post-agitation mAb solutions were examined with a DIC microscope.

Viscosity measurement of mAb solution

Purified testing human mAbs were concentrated to a desired level (ranging 70–145 mg/ml) using 10,000 MWCO Amicon Ultra-15 (Millipore) in mAb buffer. The solution viscosity was determined at each mAb concentration using a dynamic light scattering method described previously.[33] In brief, 49.5 μl of mAb samples and 0.5 μl of polystyrene beads (101.5 nm nominal radius at 1.05 g/ml density; Thermo Scientific) were mixed and the diffusion of the beads were measured with DynaPro™ plate reader (Wyatt Technology) at 25°C in a 384-well format. The solution micro-viscosity was calculated from diffusion coefficient data by applying the Stokes-Einstein equation (see ref [33] for detail).

Disclosure of Potential Conflicts of Interest

No potential conflicts of interest were disclosed.

Acknowledgments

The authors thank Rutilio Clark, Jenni Lavallee, Rick Jacobsen, Kevin Graham, Elham Ettehadieh, Shanon Turnbaugh for providing expression constructs used in this study.

Author Contributions

HH designed the work. HH, CEW, FK, FH performed the work. HH and ACL wrote the manuscript; all the authors reviewed the manuscript.

References

1. Podell DN, Packman CH, Maniloff J, Abraham GN. Characterization of monoclonal IgG cryoglobulins: fine-structural and morphological analysis. Blood 1987; 69:677-81; PMID:3801676
2. Wang Y, Lomakin A, Hideshima T, Laubach JP, Ogun O, Richardson PG, Munshi NC, Anderson KC, Benedek GB. Pathological crystallization of human immunoglobulins. Proc Nat Acad Sci U S A 2012; 109:13359-61; PMID:22847421; http://dx.doi.org/10.1073/pnas.1211723109
3. Wang Y, Lomakin A, Latypov RF, Laubach JP, Hideshima T, Richardson PG, Munshi NC, Anderson KC, Benedek GB. Phase transitions in human IgG solutions. J Chem Phys 2013; 139:121904; PMID:24089716; http://dx.doi.org/10.1063/1.4811345
4. Trilisky E, Gillespie R, Osslund TD, Vunnum S. Crystallization and liquid-liquid phase separation of monoclonal antibodies and fc-fusion proteins: screening results. Biotechnol Prog 2011; 27:1054-67; PMID:21656920; http://dx.doi.org/10.1002/btpr.621
5. Ahamed T, Esteban BN, Ottens M, van Dedem GW, van der Wielen LA, Bisschops MA, Lee A, Pham C, Thommes J. Phase behavior of an intact monoclonal antibody. Biophys J 2007; 93:610-9; PMID:17449660; http://dx.doi.org/10.1529/biophysj.106.098293
6. Hasegawa H. Aggregates, crystals, gels, and amyloids: intracellular and extracellular phenotypes at the crossroads of immunoglobulin physicochemical property and cell physiology. Int J Cell Biol 2013; 2013:604867; PMID:23533417; http://dx.doi.org/10.1155/2013/604867
7. Hall CG, Abraham GN. Reversible self-association of a human myeloma protein. Thermodynamics and relevance to viscosity effects and solubility. Biochemistry 1984; 23:5123-9; PMID:6509016; http://dx.doi.org/10.1021/bi00317a007
8. Ferri C, Zignego AL, Pileri SA. Cryoglobulins. J Clin Pathol 2002; 55:4-13; PMID:11825916; http://dx.doi.org/10.1136/jcp.55.1.4
9. Durie BG, Salmon SE. A clinical staging system for multiple myeloma. Correlation of measured myeloma cell mass with presenting clinical features, response to treatment, and survival. Cancer 1975; 36:842-54; PMID:1182674; http://dx.doi.org/10.1002/1097-0142(197509)36:3%3c842::AID-CNCR2820360303%3e3.0.CO;2-U
10. Wang Y, Latypov RF, Lomakin A, Meyer JA, Kerwin BA, Vunnum S, Benedek GB. Quantitative evaluation of colloidal stability of antibody solutions using PEG-induced liquid-liquid phase separation. Mol Pharm 2014; 11:1391-402; PMID:24679215; http://dx.doi.org/10.1021/mp400521b
11. Woodard J, Lau H, Latypov RF. Nondenaturing size-exclusion chromatography-mass spectrometry to measure stress-induced aggregation in a complex mixture of monoclonal antibodies. Anal Chem 2013; 85:6429-36; PMID:23742703; http://dx.doi.org/10.1021/ac401455f
12. Chen S, Lau H, Brodsky Y, Kleemann GR, Latypov RF. The use of native cation-exchange chromatography to study aggregation and phase separation of monoclonal antibodies. Protein Sci: Pub Protein Soc 2010; 19:1191-204; PMID:20512972; http://dx.doi.org/10.1002/pro.396
13. Manning MC, Chou DK, Murphy BM, Payne RW, Katayama DS. Stability of protein pharmaceuticals: an update. Pharm Res 2010; 27:544-75; PMID:20143256; http://dx.doi.org/10.1007/s11095-009-0045-6
14. Ronco P, Plaisier E, Mougenot B, Aucouturier P. Immunoglobulin light (heavy)-chain deposition disease: from molecular medicine to pathophysiology-driven therapy. Clin J Am Soc Nephrol: CJASN 2006; 1:1342-50; PMID:17699367; http://dx.doi.org/10.2215/CJN.01730506
15. Stoops J, Byrd S, Hasegawa H. Russell body inducing threshold depends on the variable domain sequences of individual human IgG clones and the cellular protein homeostasis. Biochimica et Biophysica Acta 2012; 1823:1643-57; PMID:22728328; http://dx.doi.org/10.1016/j.bbamcr.2012.06.015
16. Alanen A, Pira U, Lassila O, Roth J, Franklin RM. Mott cells are plasma cells defective in immunoglobulin secretion. Eur J Immunol 1985; 15:235-42; PMID:3979421; http://dx.doi.org/10.1002/eji.1830150306
17. Ronzoni R, Anelli T, Brunati M, Cortini M, Fagioli C, Sitia R. Pathogenesis of ER storage disorders: modulating Russell body biogenesis by altering proximal and distal quality control. Traffic 2010; 11:947-57; PMID:20406418; http://dx.doi.org/10.1111/j.1600-0854.2010.01071.x
18. Valetti C, Grossi CE, Milstein C, Sitia R. Russell bodies: a general response of secretory cells to synthesis of a mutant immunoglobulin which can neither exit from, nor be degraded in, the endoplasmic reticulum. J Cell Biol 1991; 115:983-94; PMID:1955467; http://dx.doi.org/10.1083/jcb.115.4.983
19. Hasegawa H, Wendling J, He F, Trilisky E, Stevenson R, Franey H, Kinderman F, Li G, Piedmonte DM, Osslund T, et al. In vivo crystallization of human IgG in the endoplasmic reticulum of engineered Chinese hamster ovary (CHO) cells. J Biol Chem 2011; 286:19917-31; PMID:21464137; http://dx.doi.org/10.1074/jbc.M110.204362
20. Fujiwara T, Oda K, Yokota S, Takatsuki A, Ikehara Y. Brefeldin A causes disassembly of the Golgi complex and accumulation of secretory proteins in the endoplasmic reticulum. J Biol Chem 1988; 263:18545-52; PMID:3192548
21. Lippincott-Schwartz J, Yuan LC, Bonifacino JS, Klausner RD. Rapid redistribution of Golgi proteins into the ER in cells treated with brefeldin A: evidence for membrane cycling from Golgi to ER. Cell 1989; 56:801-13; PMID:2647301; http://dx.doi.org/10.1016/0092-8674(89)90685-5
22. Hasegawa H, Forte C, Barber I, Turnbaugh S, Stoops J, Shen M, Lim AC. Modulation of in vivo IgG crystallization in the secretory pathway by

heavy chain isotype class switching and N-linked glycosylation. Biochimica et Biophysica Acta 2014; 1843:1325-38; PMID:24703881; http://dx.doi.org/10.1016/j.bbamcr.2014.03.024
23. Eppler A, Weigandt M, Hanefeld A, Bunjes H. Relevant shaking stress conditions for antibody preformulation development. Eur J Pharm Biopharm: Off J Arbeitsgemeinschaft fur Pharmazeutische Verfahrenstechnik eV 2010; 74:139-47; PMID:19922795; http://dx.doi.org/10.1016/j.ejpb.2009.11.005
24. Shire SJ, Shahrokh Z, Liu J. Challenges in the development of high protein concentration formulations. J Pharm Sci 2004; 93:1390-402; PMID:15124199; http://dx.doi.org/10.1002/jps.20079
25. Mehta J, Singhal S. Hyperviscosity syndrome in plasma cell dyscrasias. Semin Thromb Hemost 2003; 29:467-71; PMID:14631546; http://dx.doi.org/10.1055/s-2003-44554
26. Zlotnick A. The morular cell and the grape cell in bone marrow and peripheral blood. Blood 1956; 11:1140-7; PMID:13373931
27. Franey H, Brych SR, Kolvenbach CG, Rajan RS. Increased aggregation propensity of IgG2 subclass over IgG1: role of conformational changes and covalent character in isolated aggregates. Protein Sci: Pub Protein Soc 2010; 19:1601-15; PMID:20556807; http://dx.doi.org/10.1002/pro.434
28. Rengers JU, Touchard G, Decourt C, Deret S, Michel H, Cogne M. Heavy and light chain primary structures control IgG3 nephritogenicity in an experimental model for cryocrystalglobulinemia. Blood 2000; 95:3467-72; PMID:10828030
29. Paroutis P, Touret N, Grinstein S. The pH of the secretory pathway: measurement, determinants, and regulation. Physiol (Bethesda) 2004; 19:207-15; PMID:15304635; http://dx.doi.org/10.1152/physiol.00005.2004
30. Rutishauser J, Spiess M. Endoplasmic reticulum storage diseases. Swiss Med Weekly 2002; 132:211-22; PMID:12087487
31. Russell W. The parasite of cancer. Lancet 1899; 153:1138-41; http://dx.doi.org/10.1016/S0140-6736(00)65286-8
32. Retter I, Althaus HH, Munch R, Muller W. VBASE2, an integrative V gene database. Nucleic Acids Res 2005; 33:D671-4; PMID:15608286; http://dx.doi.org/10.1093/nar/gki088
33. He F, Becker GW, Litowski JR, Narhi LO, Brems DN, Razinkov VI. High-throughput dynamic light scattering method for measuring viscosity of concentrated protein solutions. Anal Biochem 2010; 399:141-3; PMID:19995543; http://dx.doi.org/10.1016/j.ab.2009.12.003